PHYSICAL REVIEW A **82**, 031804(R) (2010)

Cavity optomechanics with ultrahigh-Q crystalline microresonators

J. Hofer,[1] A. Schliesser,[1] and T. J. Kippenberg[1,2,*]
[1]*Max Planck Institut für Quantenoptik, D-85748 Garching, Germany*
[2]*Ecole Polytechnique Fédérale de Lausanne, CH-1015, Lausanne, Switzerland*
(Received 6 November 2009; published 23 September 2010)

We present the observation of optomechanical coupling in crystalline whispering-gallery-mode (WGM) resonators. The high purity of the material enables optical quality factors in excess of 10^{10} and finesse exceeding 10^6, as well as mechanical quality factors greater than 10^5. Ultrasensitive displacement measurements reveal mechanical radial modes at frequencies up to 20 MHz, corresponding to unprecedentedly high sideband factors (>100). In combination with the weak intrinsic mechanical damping this renders crystalline WGM microresonators promising for experiments in the classical and quantum regime of optomechanics.

DOI: 10.1103/PhysRevA.82.031804 PACS number(s): 42.65.Sf, 42.50.Wk

Optical interferometers with suspended mirrors have traditionally been key elements in gravitational wave detectors. Implemented at a mesoscopic scale ($\lesssim$1 cm), microscale and nanoscale physical systems hosting optical and mechanical degrees of freedom may allow studying optomechanical coupling at the quantum level [1,2]. In particular, recent experiments have aimed toward the observation of measurement quantum backaction [3,4] and radiation-pressure cooling of a mesoscopic mechanical oscillator to its quantum ground state [5–7]. However, inevitable coupling of the system to its environment severely impedes such studies. For example, thermal fluctuations associated with mechanical dissipation mask the signatures of quantum backaction [3,4], but also constitute a mechanism competing with radiation-pressure cooling [5–7]. Optical losses, on the other hand, destroy potential quantum correlations [3], give rise to heating due to the absorbed photons [5], and preclude reaching the important resolved-sideband regime [8]. Optomechanical systems based on amorphous materials such as SiO_2 are prone to mechanical losses due to coupling of strain fields to two-level systems (TLS) [9], particularly severe at cryogenic temperatures [10]. Strained silicon nitride oscillators have achieved higher mechanical quality factors up to 1×10^7, but optical absorption may limit the finesse in systems based on this material [11–13] due to the residual imaginary part of the refractive index amounting to $\mathrm{Im}(n) \lesssim 10^{-5}$ according to a recent report [14]. Ultrapure crystalline materials, in contrast, do generally not suffer from such restrictions. In fact, the best optical resonators available today are whispering-gallery-mode (WGM) resonators made from CaF_2, featuring $\mathcal{F}$ up to 10^7 [15–17], which corresponds to $\mathrm{Im}(n) \approx 2 \times 10^{-12}$. At the same time, due to their long-range order, these materials are ideally free from TLS leading to ultrahigh mechanical quality factors. Indeed, remarkably high values up to 4×10^9 have been reported for a 1-MHz bulk quartz oscillator at a temperature of 2 K [18].

Here, we combine the generally favorable properties of monolithic WGM optomechanical systems in terms of optomechanical coupling strength, stability, and cryogenic compatibility with a crystalline material. Following pioneering work [16,17] we fabricate crystalline WGM resonators from purest available CaF_2 or MgF_2 raw material. In brief, small cylindrical and disk preforms were drilled out of crystalline blanks and mounted onto an air-bearing spindle, which provides extremely low rotational imprecision (<100 nm). The preforms were shaped using diamond turning and, to minimize surface scattering, a polishing procedure with diamond abrasive of successively decreasing grit size (down to an average size of 25 nm) was applied.

Highly efficient evanescent coupling to crystalline WGM resonators can be achieved by the use of tapered optical fibers, providing single-mode input and output as well as tunable

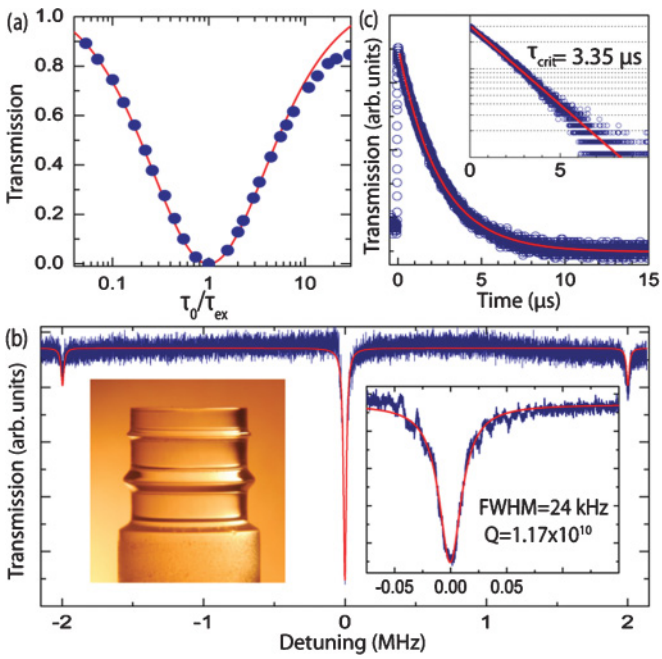

FIG. 1. (Color online) (a) Transmission on resonance vs coupling parameter τ_0/τ_{ex} while approaching a tapered fiber to a CaF_2 cavity. The data (blue circles) show that ideal coupling behavior (red line) is possible up to a coupling factor $\tau_0/\tau_{ex} \approx 8$. (b) Measurement of the resonance linewidth of a different cavity (radius 2 mm) with calibration peaks at 2 MHz detuning and Lorentzian fit (red line). The left inset shows a diamond-turned resonator made of CaF_2. (c) Ringdown measurements (blue circles) of the same resonator and exponential fit (red line). The measured lifetime of $\tau = 3.35\ \mu$s corresponds to an intrinsic quality factor of $Q_0 = 1.18 \times 10^{10}$.

*tobias.kippenberg@epfl.ch

 ©2010 The American Physical Society

coupling [19]. Depending on the size of the resonator and the used wavelength, phase matching is achieved by adjusting the taper waist radius. For the used CaF_2 resonators of radius $R = 800\,\mu$m and 2 mm, the optimum taper waist corresponds to $1.15\,\mu$m and $1.25\,\mu$m. As an example, Fig. 1(a) shows coupling to a CaF_2 resonator of 800-μm radius possessing an intrinsic optical quality factor $Q_0 = \tau_0\omega = 1.4 \times 10^9$, where τ_0 is the intrinsic photon lifetime and ω the optical carrier frequency. The coupling to the waveguide can be described by the dimensionless parameter τ_0/τ_{ex}, where τ_{ex}^{-1} reflects the photon loss rate due to coupling to the waveguide and the resulting linewidth is given by $\kappa = \tau^{-1} = \tau_0^{-1} + \tau_{ex}^{-1}$. The data clearly show that critical ($\tau_0 = \tau_{ex}$) and strong overcoupling up to $\tau_0/\tau_{ex} = 30$ are possible; however, coupling deviates from ideality [19] for $\tau_0/\tau_{ex} > 8$. Since the coupling rate τ_{ex}^{-1} is proportional to the relatively small volume overlap of the (large) WGM and the propagating taper mode, strong overcoupling is only possible for ultralow intrinsic loss rates τ_0^{-1}.

For another CaF_2 resonator (radius 2 mm), the optical quality factor was inferred both from linewidth measurements and cavity ringdown experiments. The linewidth was measured with a scanning Nd:YAG (yttrium aluminum garnet) laser at 1064 nm. In the undercoupled regime ($\tau_{ex} \gg \tau_0$) the highest measured Q factor was 1.17×10^{10}. In addition, the Q factor was independently measured using cavity ringdown, yielding a total lifetime of $\tau = 3.35\,\mu$s at critical coupling. The corresponding intrinsic cavity $Q_0 = 1.18 \times 10^{10}$ is in excellent agreement with the linewidth measurements and corresponds to an intrinsic finesse $\mathcal{F}_0 = 770\,000$. The highest value attained in such a measurement was $\mathcal{F}_0 = 1.1 \times 10^6$ for a CaF_2 resonator with a 550-μm radius. Similar values were measured with MgF_2 resonators.

WGM resonators possess inherent optomechanical coupling of the optical mode with structural mechanical resonances which displace the resonator's boundaries. We studied this ponderomotive interaction in several different resonator geometries made of CaF_2 and MgF_2. We first discuss the results of a typical milllimeter-scale CaF_2 cylindrical resonator, 8 mm in height and 2 mm radius, similar to the geometry of the resonator shown in Fig. 1(b). To detect the mechanical modes' Brownian motion, a weak beam from a cw Ti:sapphire laser was coupled to a WGM using a tapered optical fiber, and locked to the side of an optical resonance's fringe. Thermal fluctuations of the cavity radius cause changes in the optical path length, which imprint themselves into a modulation of the power transmitted past the cavity. Spectral analysis of the transmitted power thus allows extracting the mechanical frequency and dissipation rate $\Gamma_m = \Omega_m/Q_m$. Alternatively, to achieve a quantum-limited displacement sensitivity a phase-sensitive polarization spectroscopy scheme was used [8]. Using these methods, more than 20 mechanical modes with frequencies ranging from approximately 500 kHz to 2 MHz were observed. For a freely standing cylinder we obtain $Q_m \sim 20\,000$. In order to reduce the influence of clamping losses and gas friction, the resonator was mounted with four sharp tungsten tips (apex $\approx 1\,\mu$m) and measured in a low pressure environment (<10 mbar). As an example a mechanical mode with an eigenfrequency of 856 kHz is shown in Fig. 2, at atmospheric and at low pressure (with Q_m of 24 700 and 114 300, respectively). In this configuration several modes had Q factors exceeding 10^5 with a maximum Q_m of 136 000 at a frequency of 1.1 MHz. Note that this corresponds to a Q-frequency product greater than 10^{11} at room temperature. Due to the strong dependence of the measured Q_m on the device's clamping, we expect that significantly higher Q_m can be achieved by optimizing the clamping.

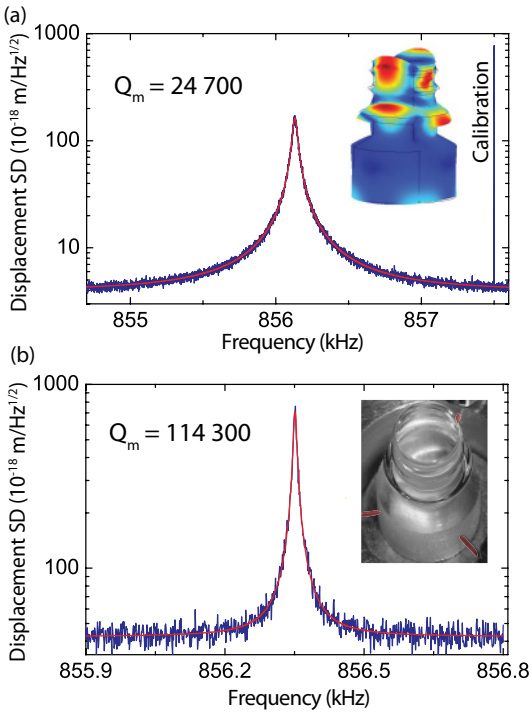

FIG. 2. (Color online) Displacement spectral density (SD) of a mechanical mode of a cylindrical cavity. (a) Cavity free-standing at atmospheric pressure. The blue lines are data (with calibration [8] peak), the red lines are Lorentzian fits. The inset shows the typical displacement pattern of a mode in this frequency range. (b) The quality factor of the same mechanical mode measured at low pressure and with optimized clamping increased to 114 300. The inset illustrates the mounting of the resonator. It is clamped by four tungsten tips, three sidewise (red shaded), and one from below.

To fully assess the performance of an optomechanical system, it is also necessary to quantify the optomechanical coupling strength, which is usually expressed in terms of the (mutually dependent) coupling parameter G and effective mass m_{eff}. The former indicates the differential frequency shift $\delta\omega$ for a given displacement x via $\delta\omega = Gx$. In complex three-dimensional structures such as those employed here, however, the definition of x (and therefore G) is indeed arbitrary. Physically, the mechanical modes (enumerated in the following with an index i) are characterized by a three-dimensional displacement field $\vec{u}_i(\vec{r})$. It can be mapped to the scalar x using a weighting function $\vec{w}(\vec{r})$ according to $x = \langle \vec{w}, \vec{u} \rangle \equiv \int \vec{w}(\vec{r}) \cdot \vec{u}(\vec{r}) d^3r$, where $\vec{u}(\vec{r}) = \sum_i \vec{u}_i(\vec{r})$. Here, the spatial distribution of $\vec{w}$ is determined by the requirement to reproduce the physically expected frequency shift Gx for any displacement pattern $\vec{u}$, and is essentially given by the optical field distribution in the locations of a gradient (or jump) in the dielectric function [20]. The normalization of $\vec{w}$, in contrast, is

only determined by the choice of the parameter G. The effective mass m_i [21,22] of the ith mode, in turn, is determined by the requirement that the potential energy upon its displacement $x_i = \langle \vec{w}, \vec{u}_i \rangle$ is given by $U_i = \frac{1}{2} m_i \Omega_i^2 x_i^2$, implying [22] that $m_i = \int \rho(\vec{r}) |\vec{u}_i(\vec{r})|^2 d^3r / \langle \vec{w}, \vec{u}_i \rangle^2$, evidently scaling quadratic in the choice of coupling constant G [$\rho(\vec{r})$ is the density]. Dropping the index i, the optomechanical interaction Hamiltonian can be written as $\hat{H}_{\rm int} = \hbar\, G\, \hat{a}_{\rm o}^\dagger \hat{a}_{\rm o}\, x_{\rm zpf}\, (\hat{a}_{\rm m}^\dagger + \hat{a}_{\rm m})$, where $\hat{a}_{\rm o}$ ($\hat{a}_{\rm o}^\dagger$) and $\hat{a}_{\rm m}$ ($\hat{a}_{\rm m}^\dagger$) are the optical and mechanical annihilation (creation) operators. Note that for each mechanical mode, the vacuum optomechanical coupling rate $G x_{\rm zpf}$ is independent of the choice of G, as $x_{\rm zpf} = \sqrt{\hbar/(2 m_{\rm eff} \Omega_{\rm m})}$.

In the case of WGM optomechanical systems, a natural choice for the optomechanical coupling is given by $G = -\omega/R$, mapping the displacement fields to an effective change in the radius of the entire structure. From room-temperature measurements, we can then experimentally derive the effective mass from the calibrated [8] displacement spectra $\bar{S}_{xx}(\Omega)$ using the relation $\bar{S}_{xx}(\Omega_i) = 2 k_{\rm B} T/(m_i \Omega_i^2 \Gamma_i)$. The effective masses measured in this manner on the cylindrical samples are still comparably high (~50 mg). However, as we show here, it can be dramatically reduced by fabricating disk-shaped crystalline resonators. To this end, we fabricated a CaF_2 resonator of 100-μm thickness and 800-μm radius, corresponding to a optomechanical coupling constant $|G/2\pi| = 350$ MHz/nm. The magnitude of the intrinsic optical Q factor of the disk was 1.4×10^9 and mechanical modes were measured with a Nd:YAG laser locked to the side of a cavity resonance, which allowed a shot-noise limited displacement sensitivity at the level of 1×10^{-18} m/$\sqrt{\rm Hz}$ above 6 MHz. Below 6 MHz the sensitivity was limited by classical laser noise, which was characterized using an independent fiber loop cavity. In a first measurement the CaF_2 disk was waxed on a metal holder that was used in the fabrication process. Besides the high-Q modes ($Q_{\rm m}$ up to 15 000), the most prominent feature in the noise spectrum as shown in Fig. 3(a) are three broad Lorentzian peaks which can be attributed to different orders of radial breathing modes [(RBMs), $Q_{\rm m} < 100$] with effective masses from 400 to 700 μg. Note that in addition to the low mass the frequency of these modes falls in the range greater than 10 MHz and therefore provides hereto unprecedented sideband factors ($\Omega_{\rm m}/\kappa > 100$). To reduce coupling of the RBMs to the environment, the disk was clamped centrally between two sharp tungsten tips, which led to a substantial increase of the Q factor, most distinct for lower-order RBMs. While for the first-order RBM a quality factor of 2500 was measured in this configuration, it was 300, 70, and 40 for second, third, and fourth orders, respectively, limited by clamping losses as explained below.

To verify the nature of the observed modes we used finite element modeling (COMSOL Multiphysics). CaF_2 is a cubic crystal and described by three independent elastic constants. Taking into account the crystalline orientation (symmetry axis of the resonator parallel to [111]), and appropriate boundary conditions, the mechanical eigenfrequencies, mode energies, and stress and strain fields were inferred from the simulation. Three-dimensional simulations yield very accurate values for the mode frequencies but also a dense mode spectrum (~20 modes per MHz). Most of the modes with small masses

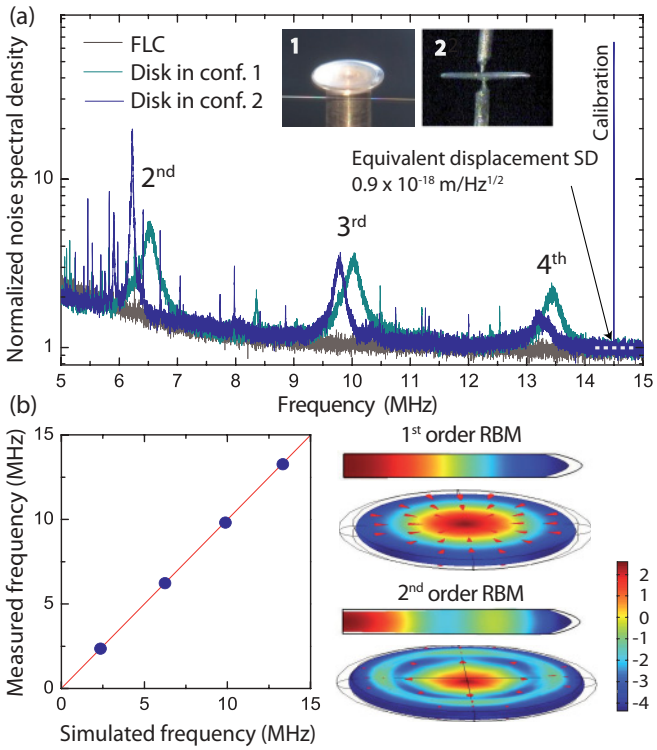

FIG. 3. (Color online) (a) Photocurrent spectral density normalized to equivalent mechanical displacement fluctuations at a Fourier frequency of 14.5 MHz. Three spectra were measured with a Nd:YAG laser coupled to a CaF_2 microdisk waxed on a metal holder (configuration 1), the same disk clamped between two tungsten tips (configuration 2), and a fiber loop cavity (FLC). The disk exhibits several orders of mechanical radial breathing modes (RBMs) up to 20 MHz (second to fourth order are shown). (b) For the case of central clamping, measurement and simulation of first- to fourth-order RBM frequencies show excellent agreement. The increase in modal displacement at the support tip for higher-order RBMs explains the measured dependence of $Q_{\rm m}$ on the RBM order (from $Q_{\rm m} = 2500$ to $Q_{\rm m} = 40$). The color code represents radial displacement (arbitrary units).

can already be identified in a two-dimensional model exploiting the cylindrical symmetry of the boundary conditions. For the case of central clamping between two sharp tips, a stress-free boundary condition was applied and matching of measured and simulated frequencies of first- to fourth-order RBM with an accuracy of better than $\pm 1\%$ was achieved. The simulated mechanical displacement fields $\vec{u}_i(\vec{r})$ also provide a way to numerically estimate the effective mass of radially symmetric modes: Approximating the weighting function by a circle of radius R, we extract the radial displacement x_i of a given radially symmetric mode at the rim of the resonator and directly solve for the effective mass using the mode's known resonance frequency and energy U_i. Indeed, measured and simulated RBM effective masses show good agreement ($\pm 10\%$). FEM was also used to identify modal patterns and the origin of clamping losses. As stated above, the Q factor in the case of central clamping strongly decreases with increasing order of the RBM. With the FEM simulation this effect can be clearly understood by the rising axial displacement at the central point for higher-order RBMs, which leads to stronger

coupling and dissipation to the environment via the tungsten support tip.

In summary, we have observed and characterized optomechanical coupling in crystalline WGM resonators, possessing both high optical and mechanical Q factors. Moreover, unprecedented sideband factors (>100) are attained, and means to reduce effective mass and clamping losses demonstrated using a disk-shaped resonator. The reported mechanical quality factors are far from material limited; as a reference value $Q_m = 3 \times 10^8$ was measured in CaF_2 at a frequency of 40 kHz and 60 K [23]. Nonetheless, the systems presented here should allow the observation of radiation-pressure induced parametric instability [24] and compare favorably to systems suggested to observe optomechanically induced quantum correlations [3]. The strong increase of the quality factor at low temperatures is in stark contrast to the universal degradation of Q_m in amorphous glass [9], limiting optomechanical cooling experiments [5,6]. The resonators can be further miniaturized down to a few tens of micrometers using diamond turning [17]. For example, an 80-μm-diam, 10-μm-thick CaF_2 disk would possess $m_{\mathrm{eff}} = 90$ ng and $\Omega_m = 63$ MHz. If $Q_m = 10^7$ can be reached, the power required to cool such a device from 1.6 K to $T = \frac{\hbar\Omega_m}{k_B}$ is only 100 μW in the resolved-sideband regime [8]. Heating due to absorbtion is likely to be totally negligible considering the optical quality of the crystal. Beyond cooling, in the regime of the parametric instability, this system may serve as a low-noise photonic rf oscillator [25], due to its high Q factor. The crystalline resonators can also operate in the regime where despite a high mechanical Q factor (>1000) the mechanical dissipation rate Γ_m can exceed κ. Pumping the cavity on the upper sideband would lead to optical gain and eventually the emission of a Stokes wave at a frequency of $\omega - \Omega_m$. In this regime, the recently analyzed [26] analogon of an optomechanical Brillouin laser can be realized.

We thank A. Matkso and M. L. Gorodetsky for valuable comments. This work was supported by the EU program MINOS and an ERC Starting Grant (SiMP). The authors acknowledge support of the Max Planck Institute of Quantum Optics.

[1] T. J. Kippenberg and K. Vahala, Science **321**, 1172 (2008).
[2] K. C. Schwab and M. L. Roukes, Phys. Today **58**, 36 (2005).
[3] P. Verlot, A. Tavernarakis, T. Briant, P.-F. Cohadon, and A. Heidmann, Phys. Rev. Lett. **102**, 103601 (2009).
[4] G. Anetsberger *et al.*, Nat. Phys. **5**, 909 (2009).
[5] A. Schliesser *et al.*, Nat. Phys. **5**, 509 (2009).
[6] Y.-S. Park and H. Wang, Nat. Phys. **5**, 489 (2009).
[7] S. Gröblacher *et al.*, Nat. Phys. **5**, 485 (2009).
[8] A. Schliesser, R. Riviere, G. Anetsberger, O. Arcizet, and T. J. Kippenberg, Nat. Phys. **4**, 415 (2008).
[9] R. O. Pohl, X. Liu, and E. Thompson, Rev. Mod. Phys. **74**, 991 (2002).
[10] O. Arcizet, R. Riviere, A. Schliesser, G. Anetsberger, and T. J. Kippenberg, Phys. Rev. A **80**, 021803 (2009).
[11] P. E. Barclay, K. Srinivasan, B. L. O. Painter, and H. Mabuchi, Appl. Phys. Lett. **89**, 131108 (2006).
[12] J. D. Thompson *et al.*, Nature (London) **452**, 72 (2008).
[13] M. Eichenfeld, R. Camacho, K. V. J. Chan, and O. Painter, Nature (London) **459**, 550 (2009).
[14] D. J. Wilson, C. A. Regal, S. B. Papp, and H. J. Kimble, Phys. Rev. Lett. **103**, 207204 (2009).
[15] A. A. Savchenkov, A. B. Matsko, V. S. Ilchenko, and L. Maleki, Opt. Express **15**, 6768 (2007).
[16] I. S. Grudinin, V. S. Ilchenko, and L. Maleki, Phys. Rev. A **74**, 063806 (2006).
[17] I. S. Grudinin *et al.*, Opt. Commun. **265**, 33 (2006).
[18] A. G. Smagin, Prib. Tekh. Eksp. **17**, 143 (1974).
[19] S. M. Spillane, T. J. Kippenberg, O. J. Painter, and K. J. Vahala, Phys. Rev. Lett. **91**, 043902 (2003).
[20] S. G. Johnson *et al.*, Phys. Rev. E **65**, 066611 (2002).
[21] A. Gillespie and F. Raab, Phys. Rev. D **52**, 577 (1995).
[22] M. Pinard, Y. Hadjar, and A. Heidmann, Eur. Phys. J. D **7**, 107 (1999).
[23] R. Nawrodt *et al.*, Eur. Phys. J. Appl. Phys. **38**, 53 (2007).
[24] T. J. Kippenberg, H. Rokhsari, T. Carmon, A. Scherer, and K. J. Vahala, Phys. Rev. Lett. **95**, 033901 (2005).
[25] K. J. Vahala, Phys. Rev. A **78**, 023832 (2008).
[26] I. S. Grudinin, H. Lee, O. Painter, and K. J. Vahala, Phys. Rev. Lett. **104**, 083901 (2010).